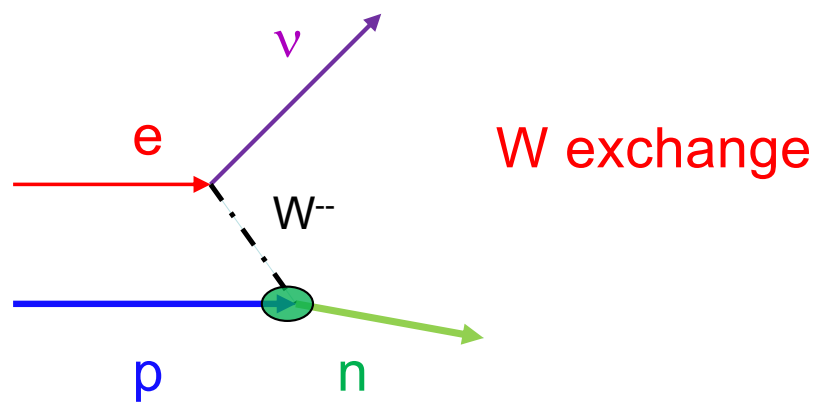


How to measure the proton weak form factor?

Bogdan Wojtsekhowski, Jefferson Lab



Weak Form Factors

Eur. Phys. J. A (2022) 58:206
<https://doi.org/10.1140/epja/s10050-022-00848-x>

THE EUROPEAN
 PHYSICAL JOURNAL A



Regular Article - Theoretical Physics

Nucleon axial form factor at large momentum transfers

Chen Chen^{1,2,a}, Craig D. Roberts^{3,4,b}

¹ Interdisciplinary Center for Theoretical Study, University of Science and Technology of China, Hefei 230026, Anhui, China

² Peng Huanwu Center for Fundamental Theory, Hefei 230026, Anhui, China

³ School of Physics, Nanjing University, Nanjing 210093, Jiangsu, China

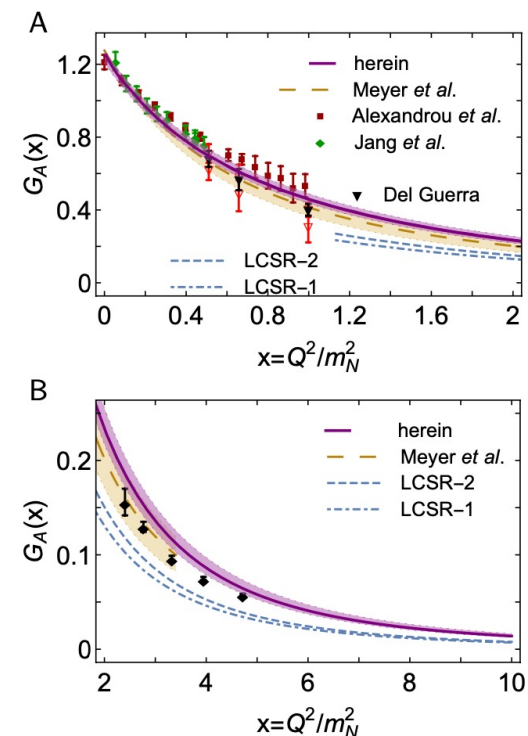
⁴ Institute for Nonperturbative Physics, Nanjing University, Nanjing 210093, Jiangsu, China

Received: 26 June 2022 / Accepted: 4 October 2022

The nucleon's axial current is also characterised by two form factors:

$$J_{5\mu}^j(K, Q) := \langle N(P_f) | \mathcal{A}_{5\mu}^j(0) | N(P_i) \rangle \quad (1a)$$

$$= \bar{u}(P_f) \frac{\tau^j}{2} \gamma_5 \left[\gamma_\mu G_A(Q^2) + \frac{iQ_\mu}{2m_N} G_P(Q^2) \right] u(P_i), \quad (1b)$$



Reference papers

NEUTRINO REACTIONS AT ACCELERATOR ENERGIES

C.H.LLEWELLYN SMITH

1972

Stanford Linear Accelerator Center, Stanford University, Stanford, California 94305, USA

The reaction $e^- + p \rightarrow \nu_e + n$ at intermediate-energies

S.L. Mintz (Florida Intl. U.), M.A. Barnett (Florida Intl. U.), G.M. Gerstner (Florida Intl. U.), M. Pourkaviani (MP Consulting, Altamonte Springs)

Mar, 1997

1996

9 pages

Published in: *Int.J.Mod.Phys.E* 6 (1997) 111-119

At first glance the reaction $e^- + p \rightarrow \nu_e + n$ might seem an unlikely one for calculation in support of possible experimental work. Because both final state particle, the neutrino and the neutron, are neutral, the reaction on the face of it would seem to be very difficult to observe. However we have been assured by experimentalists¹ that it is now very possible to observe this reaction by detecting the outgoing neutron.

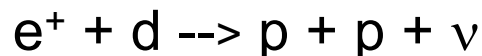
The reaction itself offers a number of advantages over other weak electron scattering reactions²⁻⁴ which have been proposed for possible experiments at facilities such as CEBAF.

2003 LOI to PAC25 by A.Deur 2023 LOIs to PAC51: one by A.Deur and a second by D.Datta

In LOI 2003 the focus was on $Q^2 \sim 1-3 \text{ GeV}^2$. Interest is large, some questions about how to proceed

In LOI 2023 AD made focus on low Q^2 , low beam energy so the pion can not be produced

DD proposed a different idea (also for low Q^2) based on TDIS proton detector and the reaction with a positron beam:



Cross section calculation

Paper by L-Smith

$$\frac{d\sigma}{d|q^2|} \left(\begin{array}{c} \nu n \rightarrow \ell^- p \\ \bar{\nu} p \rightarrow \ell^+ n \end{array} \right) = \frac{M^2 G^2 \cos^2 \theta_c}{8\pi E_\nu^2} \left[A(q^2) + B(q^2) \frac{(s-u)}{M^2} + \frac{C(q^2)(s-u)^2}{M^4} \right] (s-u = 4ME_\nu + q^2 - m^2).$$

$$A = \frac{(m^2 - q^2)}{4M^2} \left[\left(4 - \frac{q^2}{M^2} \right) |F_A|^2 - \left(4 + \frac{q^2}{M^2} \right) |F_V^1|^2 - \frac{q^2}{M^2} |\xi F_V^2|^2 \left(1 + \frac{q^2}{4M^2} \right) - \frac{4q^2 \operatorname{Re} F_V^{1*} \xi F_V^2}{M^2} \right. \\ \left. + \frac{q^2}{M^2} \left(4 - \frac{q^2}{M^2} \right) |F_A^3|^2 - \frac{m^2}{M^2} \left(|F_V^1 + \xi F_V^2|^2 + |F_A + 2F_P|^2 + \left(\frac{q^2}{M^2} - 4 \right) (|F_V^3|^2 + |F_P|^2) \right) \right] \quad (3.22)$$

$$B = -\frac{q^2}{M^2} \operatorname{Re} F_A^* (F_V^1 + \xi F_V^2) - \frac{m^2}{M^2} \operatorname{Re} \left[\left(F_V^1 + \frac{q^2}{4M^2} \xi F_V^2 \right)^* F_V^3 - \left(F_A + \frac{q^2 F_P}{2M^2} \right)^* F_A^3 \right]$$

$$C = \frac{1}{4} \left(|F_A|^2 + |F_V^1|^2 - \frac{q^2}{M^2} \left| \frac{\xi F_V^2}{2} \right|^2 - \frac{q^2}{M^2} |F_A^3|^2 \right).$$

Cross section calculation

Paper by L-Smith

$$\frac{d\sigma}{dq^2} \left(\begin{array}{c} \nu n \rightarrow \ell^- p \\ \bar{\nu} p \rightarrow \ell^+ n \end{array} \right) = \frac{M^2 G^2 \cos^2 \theta_c}{8\pi E_\nu^2} \left[A(q^2) + B(q^2) \frac{(s-u)}{M^2} + \frac{C(q^2)(s-u)^2}{M^4} \right]$$
$$(s-u = 4ME_\nu + q^2 - m^2).$$

C.H. Llewellyn Smith, Neutrino reactions at accelerator energies

303

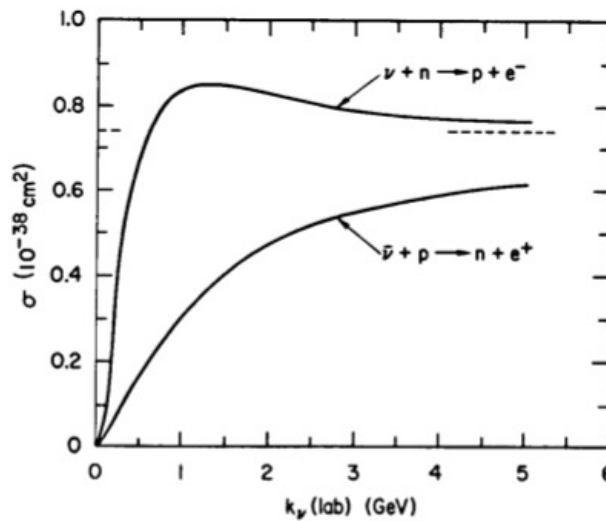


Fig. 10. Cross sections for the quasielastic process in the conventional theory with $m = 0$ and dipole forms $F(0)/(1 - q^2/0.73 \text{ GeV}^2)^2$ for the form factors F_A and $F_V^{1/2}$ [L12] (the dotted line is the limit for σ_ν and $\sigma_{\bar{\nu}}$ as $E \rightarrow \infty$).

Cross section calculation

In LOI by A.Deur

$$\frac{d\sigma}{d\omega'} = M \frac{G^2 \cos^2 \theta_c}{\pi} \frac{\omega'}{\omega} \left[\cos^2(\theta_l/2) f_2 + \left(2f_1 + \frac{\omega+\omega'}{M} f_3 \right) \sin^2(\theta_l/2) \right]$$

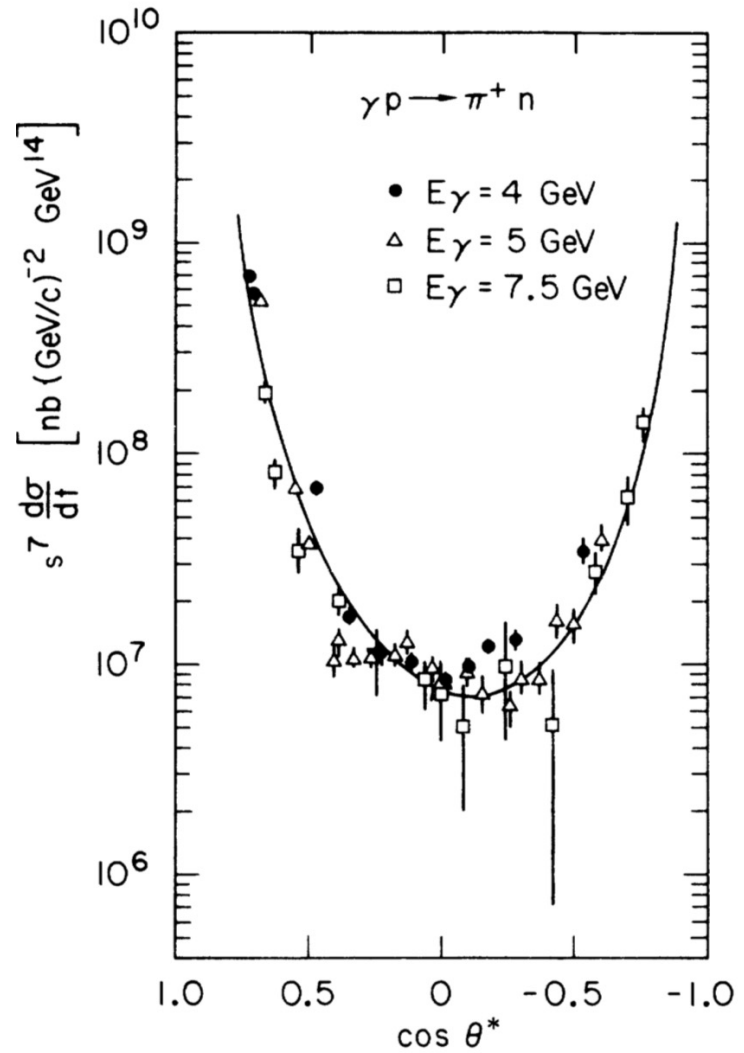
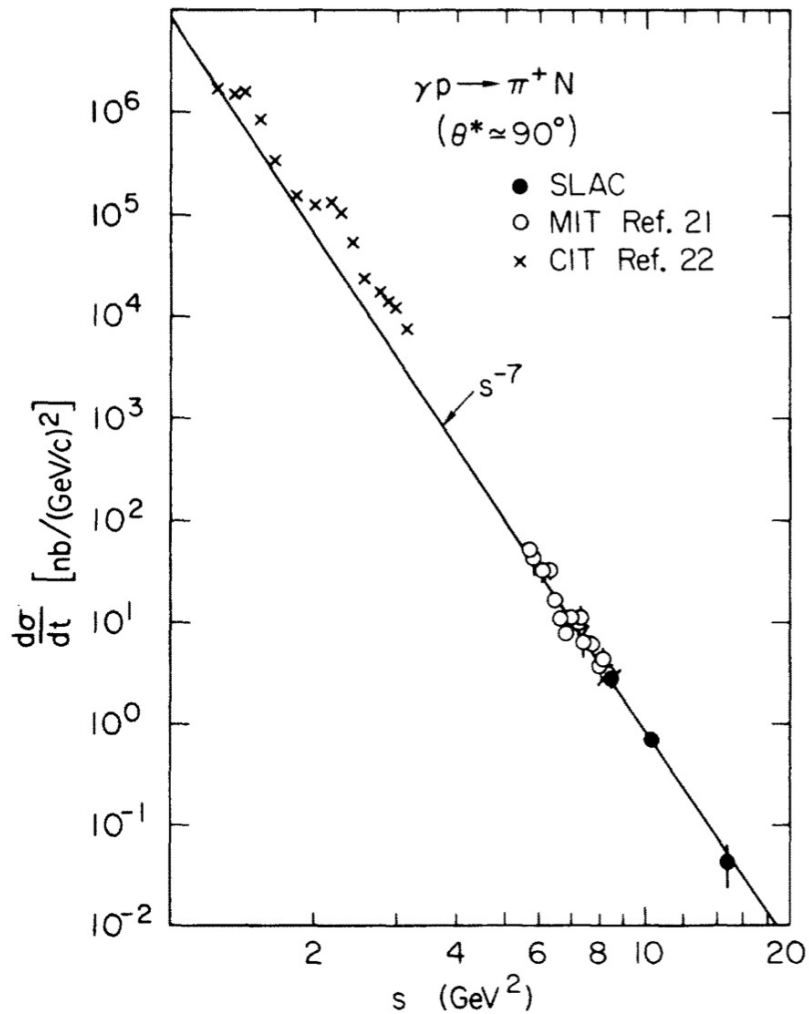
In paper by S.Mintz

$$\frac{d\sigma}{d\Omega} = \frac{m_e m_\nu G^2 M_f p_f |M|^2}{(2\pi)^2 E 8 |M_i + E - \frac{E E_f \cos \theta}{p_f}|}$$

Big challenges in the study of $e + p \rightarrow \nu + n$ process

- Cross section for the weak process is of a few $10^{-40} \text{ cm}^2/\text{sr}$
- Pion photo-production cross section $\sim 10^8$ of the weak one
- Proton rate from electron elastic e-p $\sim 10^6$ of the weak one

Pion photo production cross section



Proposed solution for the $e + p \rightarrow \nu + n$ experiment

1. High momentum resolution neutron detector
2. High angular resolution neutron detector
3. Reconstruction of the incident lepton energy to 1%
4. High efficiency of the charge particle rejection in BB
5. Analysis of the distribution (3.) shape for tagged events
6. Determination of the extra rate at the elastic “peak”

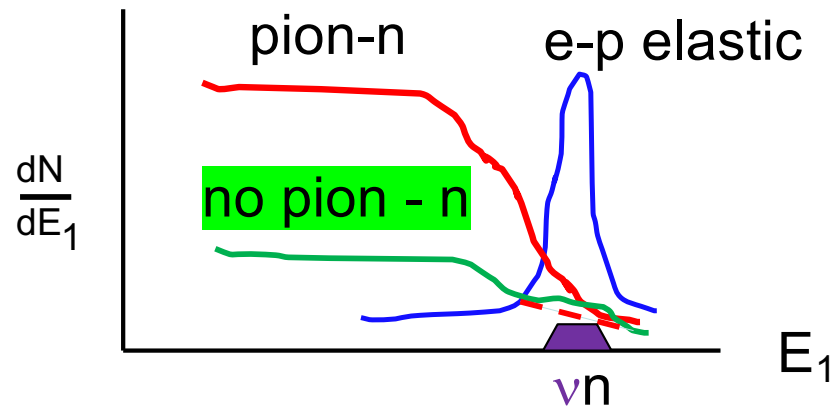
Weak Proton Form Factor at 1 GeV²

Estimation of the experiment parameters:

- Beam energy 2.2 GeV with a LH2 target
- Electron/pion/neutrino angle 54 degrees
- Recoil proton/neutron 30 degrees, $p_n = 1 \text{ GeV}/c$
- π^+ in BigBite; efficiency $\sim 95\% + 4\%$ (μ are forward)
- Electron in BigBite: efficiency 99.9%; solid angle 60 msr
- Neutron in LND: 1m x 1m, solid angle 40 msr; $\delta\theta \sim 1\text{ mrad}$
- Initial lepton momentum reconstruction accuracy $\sim 1\%$
- Photon flux $0.02 \times 1/100 \times 1/4(?) \Rightarrow 0.5/10^4$ per electron
- Electron-proton luminosity 10 cm LH2 x 100 uA = 3×10^{38}
- Rate of elastic ep events 6 kHz
- Rate of $\text{no}(e)p$ events 6 Hz, $\text{no}(e)n < 0.6 \text{ Hz}$ or $< 2k$ per hour
- Rate of π^+n events 15 Hz
- Rate of $\text{no}(\pi^+)n$ events 500 per hour
- Rate of “weak” neutrons 110 per hour
- Signal/Background 1/20 at location of the elastic “peak”
- 100 hours, 10% neutron efficiency (free protons only):
S/B = 0.050 +/- 0.01

Lepton initial energy

$$E_1 = (E_n - m) / \left[1 + \frac{P_n \cos \theta_n - E_n}{m} \right]$$



- Signal/Background 1/20 at location of the elastic “peak”
- 100 hours, 10% neutron efficiency (free protons only):

S/B = 0.050 +/- 0.01

Time-of-Flight resolution

$$\frac{\sigma_p}{p} = \gamma^2 \times \frac{\sigma_\beta}{\beta}$$

$$\frac{\sigma_\beta}{\beta} = \frac{\sigma_{ToF}}{ToF}$$

for 10 m path and 0.12 ns time resolution

using $Q^2=1$ GeV 2 ($\gamma=1.5$)

$$\frac{\sigma_p}{p} = \gamma^2 \times 1/275 \sim 0.4\%$$

0.12 ns time resolution is hard

Traditional ToF system

Number of channels $\sim 25 \times (1\text{m} \times 1\text{m}) \times 0.5\text{m}$
using 5 cm x 5 cm x 100 cm bars \rightarrow 5000 bars

With 25 m distance it will allow 40 msr solid angle

Angular resolution ~ 1 mrad

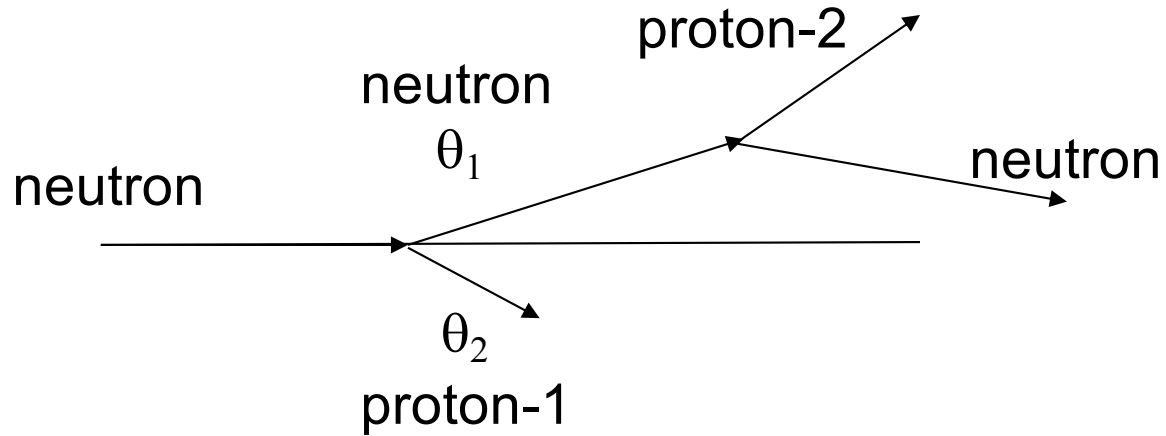
Cost per bar $\sim \$2\text{k}$ for 2 PMT + scintillator
Cost of HV+DAQ per bar $\sim \$2\text{k}$

CH, aver. density 0.79 g/cm³

1 m long detector with 0.25 ns resolution

Cost is high $\sim \$20\text{M}$

Neutron/proton tracking detector



$$E = \frac{2mc^2}{\tan \theta_1 \tan \theta_2} - mc^2$$

Mostly sensitive to the sum $(\theta_1 + \theta_2)$

for $E = 1.5 mc^2$

$$\frac{\sigma_p}{p} = 8 \times \sigma_\theta [\text{rad}] \Rightarrow 0.8\% \text{ with } 1 \text{ mrad angular resolution}$$

Scintillator fiber systems

Scintillating fiber detectors for the HypHI project at GSI

D. Nakajima^{a,b,*}, B. Özel-Tashenov^{a,c,**}, S. Bianchin^a, O. Borodina^{a,d}, V. Bo
M. Kavatsyuk^e, S. Minami^a, C. Rappold^{a,f}, T.R. Saito^{a,d}, P. Achenbach^d, S. A
T. Fukuda^h, Y. Hayashiⁱ, T. Hiraiwaⁱ, J. Hoffmann^a, K. Koch^a, N. Kurz^a, O. I
Y. Mizoi^h, T. Mochizuki^k, M. Moritsuⁱ, T. Nagaeⁱ, L. Nungesser^d, A. Okamui^a
A. Sakaguchi^k, M. Sakoⁱ, C.J. Schmidt^a, H. Sugimuraⁱ, K. Tanidaⁱ, M. Träger^a

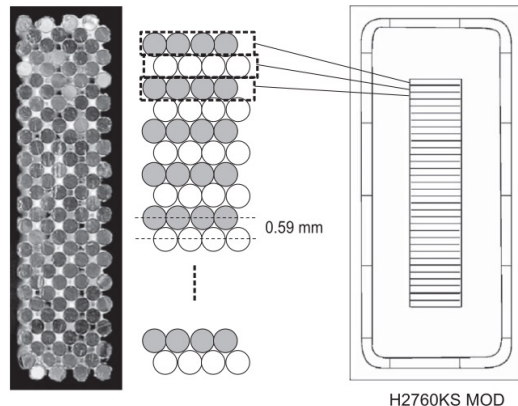
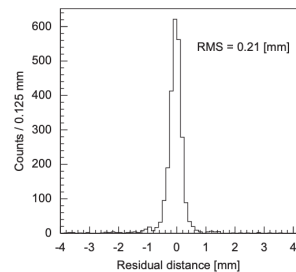


Fig. 2. (a) Cross-section of a 32-channel fiber bundle and (b) corresponding enlarged schematic drawing. The panel (c) shows a scheme of the surface of PMT H7260KS MOD.



A two-dimensional scintillation-based neutron detector with wavelength-shifting fibers and incorporating an interpolation method

T. Nakamura^{a,*}, K. Toh^a, T. Kawasaki^a, M. Ebine^b, A. Birumachi^b, K. Sakasai^a, K. Soyama^a

3.3. Spatial resolution

Fig. 7 shows the spatial resolution measured while scanning the collimated beam over the detector. The spatial responses were fitted with a Gaussian function to extract the variance (σ) for each incidence position. The spatial resolution, which was calculated as the full width at half maximum (FWHM) by 2.35σ , was better when the neutron beam was incident on top or near the WLS fiber than when it was incident between the fibers. Measurements made over a distance of 10 mm revealed a periodicity in the spatial resolution of 2.5 mm for all of the MPC logics, which reflected the pitch of the WLS fibers. These observations were consistent with the spatial responses shown in Figs. 4 and 5.

The average FWHM spatial resolutions were 3.3 ± 0.3 , 2.7 ± 0.1 , and 2.5 ± 0.1 mm for standard-, half-, and quarter-pitch logics, respectively. The spatial resolution improved from 1.2- to 1.3-fold

noise. At a single photon threshold the SiPM suffers from the same problems as a GAPD. Current state of the art SiPMs have thermal noise rates⁶ at $\mathcal{O}(100 \text{ kHz})^7$ at single photon level. This value depends on the temperature and the bias voltage. The typical pixel sizes of SiPMs are between $25 \times 25 \mu\text{m}^2$ and $100 \times 100 \mu\text{m}^2$. One single device can cover active areas up to $6 \times 6 \text{ mm}^2$ (fig. 3.9).

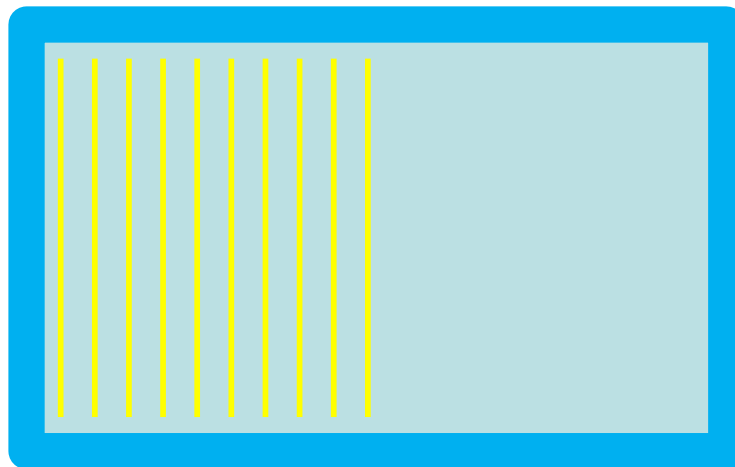
Scintillator fiber scheme

Number of channels $\sim 1\text{m} \times 1\text{m} \times 2\text{m}$ box = $500 \times 2 \times 100 = 10^5$

For 2 mm pitch X/Y and 100 layers

Cost per channel $\sim \$5$, total system $\sim \$1\text{-}2\text{M}$

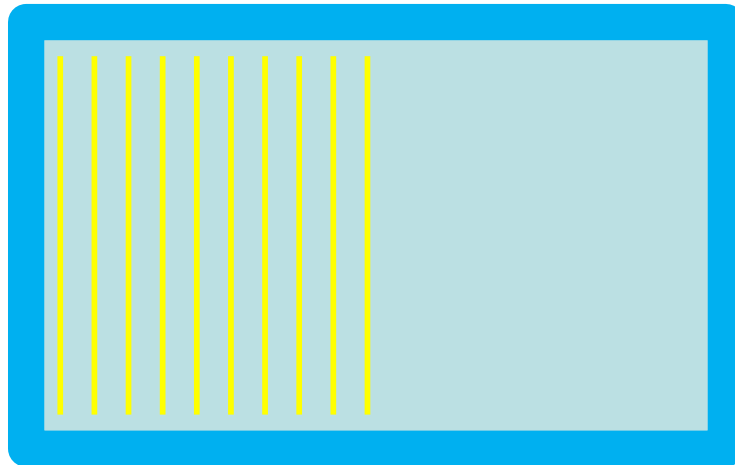
CH, aver. density 0.79 g/cm^3 ; **1/7 free protons**



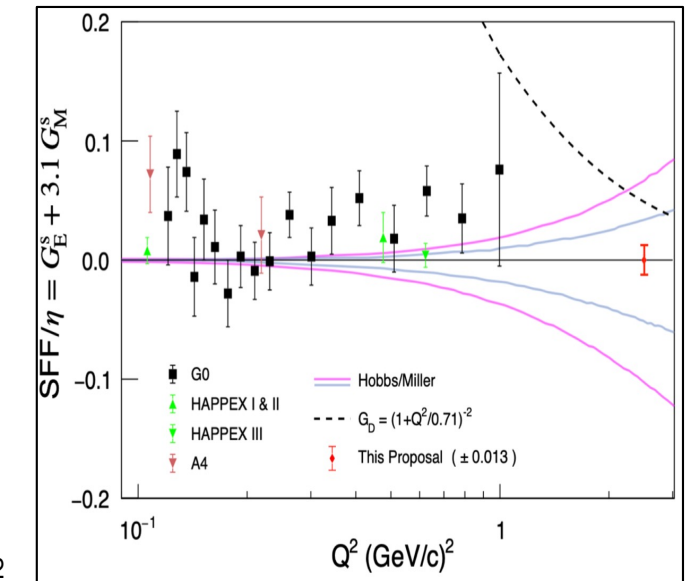
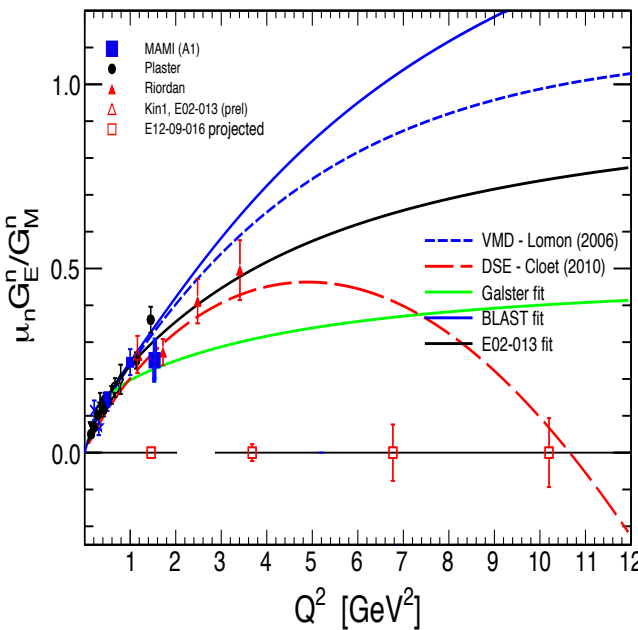
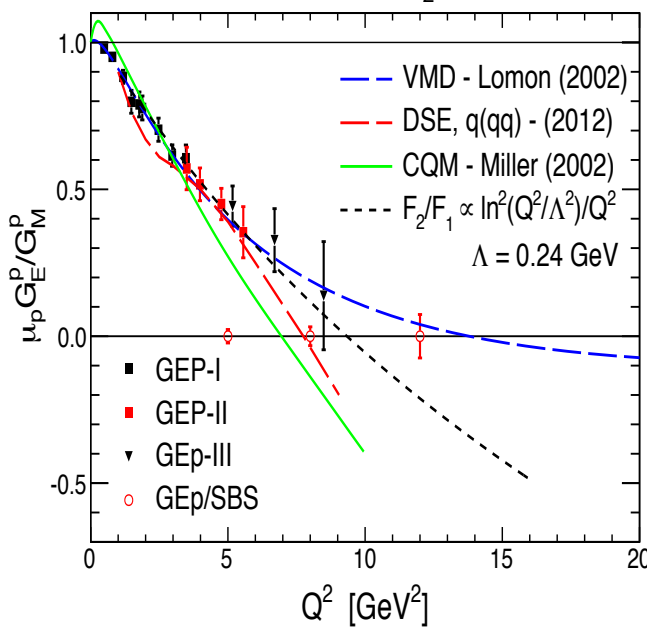
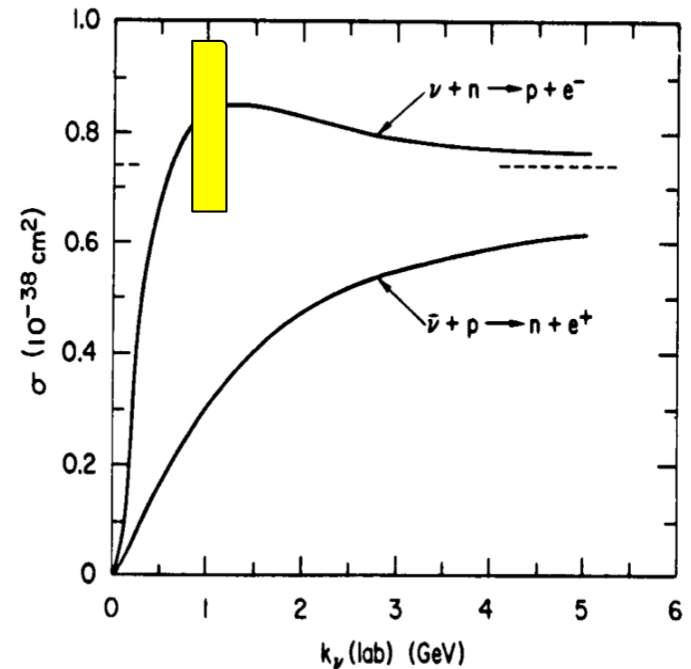
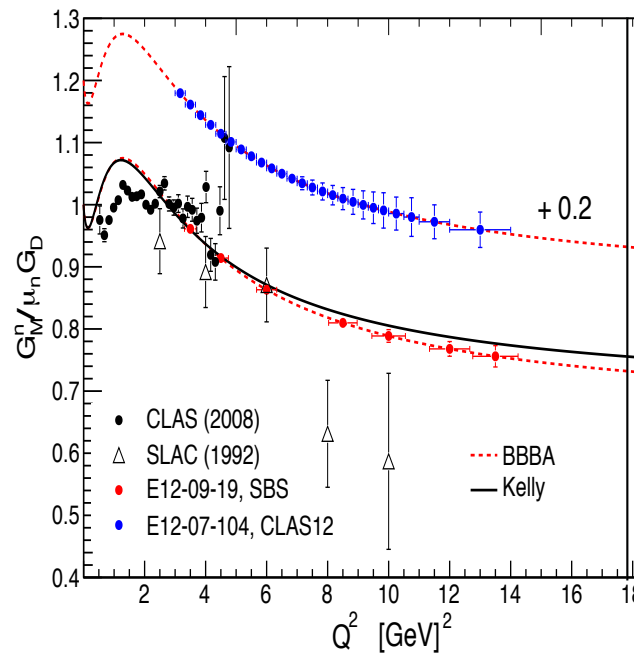
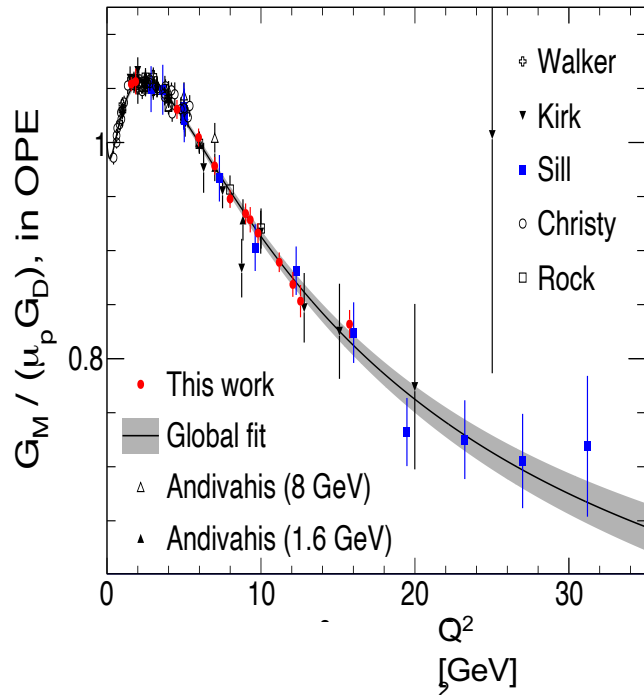
Liquid CH₄ with inserted GEM or MWPC planes

Liquid CH₄, density 0.82 g/cm³; **4/10 of free protons**

This option requires a detector expert and lot of R&D

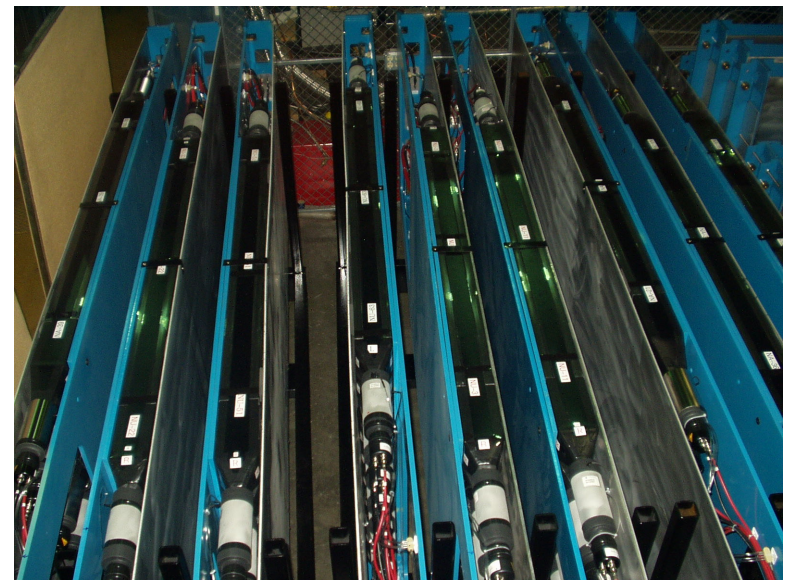
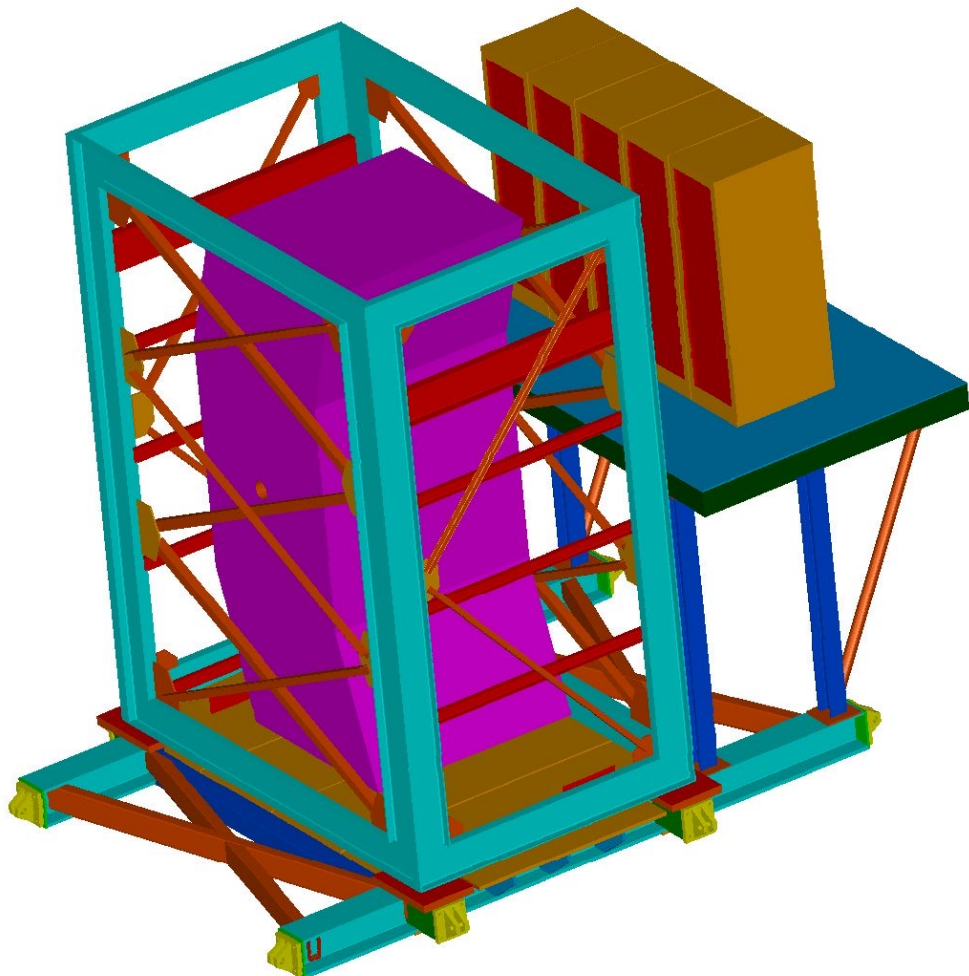


The nucleon FFs



backup

Neutron arm in GEn-I

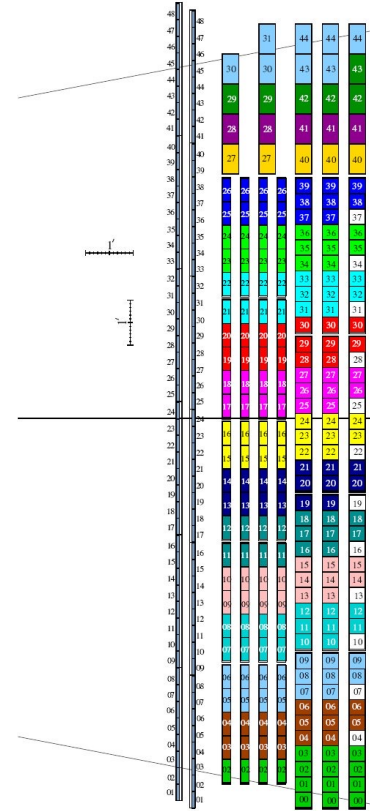
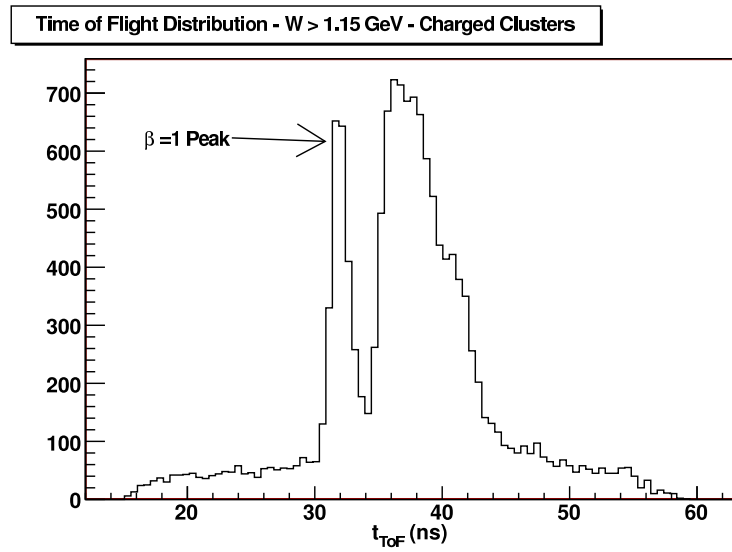
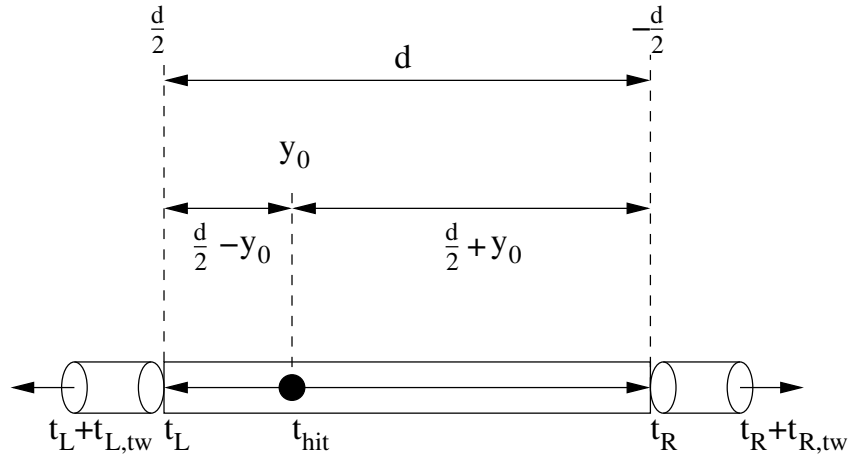


GEn-I neutron arm

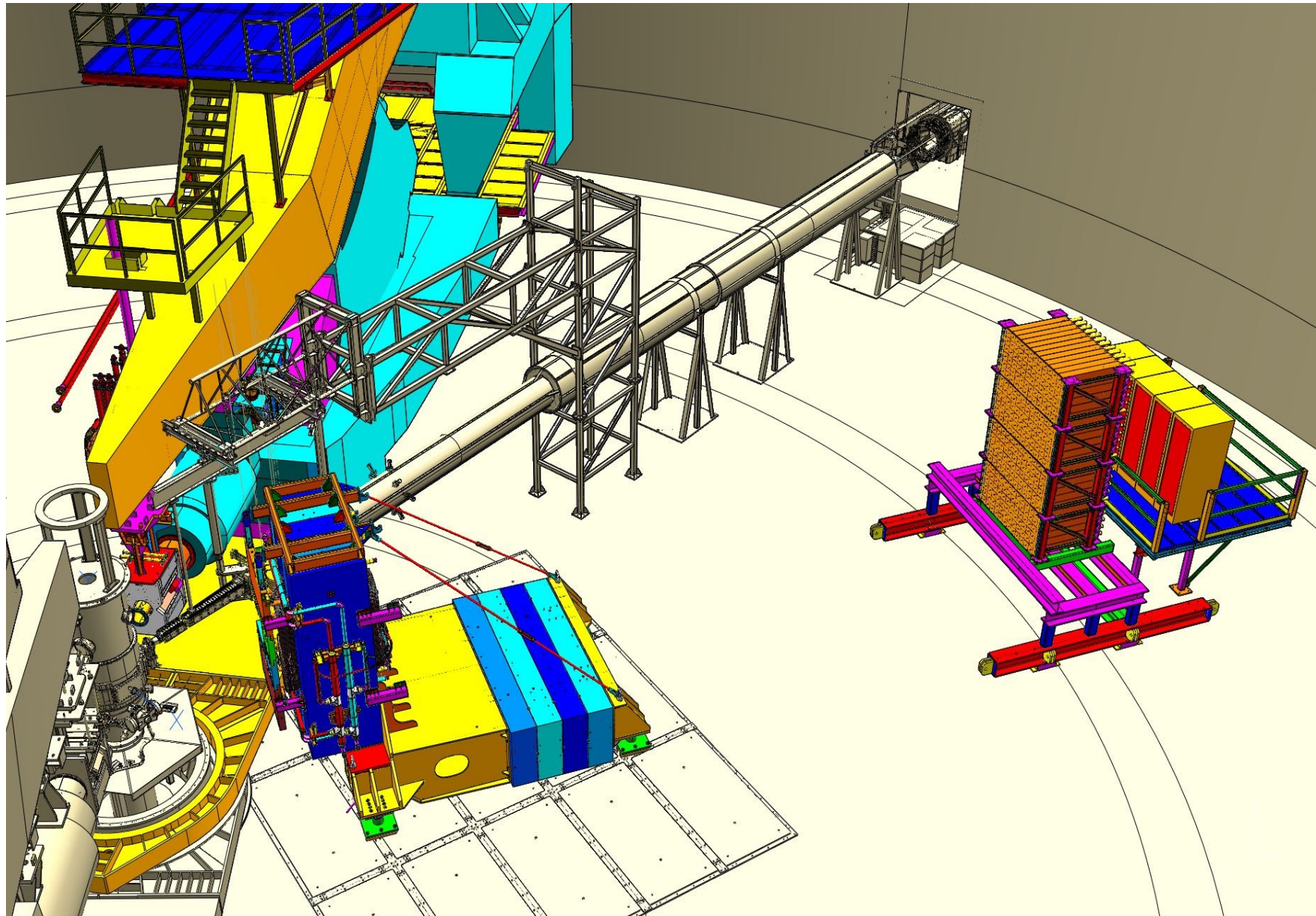


200 veto counters, ~300 neutron bars; ~800 PMTs

Time-of-flight



SBS neutron arm



SBS neutron arm

